Persistently active cannabinoid receptors mute a subpopulation of hippocampal interneurons

Attila Losonczy*, Ágota A. Biró, and Zoltan Nusser*

Laboratory of Cellular Neurophysiology, Institute of Experimental Medicine, Hungarian Academy of Sciences, 43 Szigony Street, 1083, Budapest, Hungary

Edited by Roger A. Nicoll, University of California, San Francisco, CA, and approved December 4, 2003 (received for review July 28, 2003)

Cortical information processing requires an orchestrated interaction between a large number of pyramidal cells and albeit fewer, but highly diverse GABAergic interneurons (INs). The diversity of INs is thought to reflect functional and structural specializations evolved to control distinct network operations. Consequently, specific cortical functions may be selectively modified by altering the input-output relationship of unique IN populations. Here, we report that persistently active cannabinoid receptors, the site of action of endocannabinoids, and the psychostimulants marijuana and hashish, switch off the output (mute) of a unique class of hippocampal INs. In paired recordings between cholecystokinin-immunopositive, mossy fiber-associated INs, and their target CA3 pyramidal cells, no postsynaptic currents could be evoked with single presynaptic action potentials or with repetitive stimulations at frequencies <25 Hz. Cannabinoid receptor antagonists converted these ''mute'' synapses into high-fidelity ones. The selective muting of specific GABAergic INs, achieved by persistent presynaptic cannabinoid receptor activation, provides a state-dependent switch in cortical networks.

hippocampus | inhibition | patch-clamp

Information processing in the hippocampal neuronal network relies on precise, spatiotemporal reciprocal interactions between apparently homogeneous pyramidal cells (PCs) and highly diverse GABAergic interneurons (INs) (1–5). The impact of these nerve cells on their postsynaptic target cells is determined by a variety of factors, including the number and location of synapses on the postsynaptic cell, quantal size, probability of transmitter release (P_r), and short- or long-term synaptic plasticity (6). Many of these factors are highly variable at hippocampal glutamatergic synapses (7, 8), despite the apparent uniformity of PCs. In contrast, at GABAergic synapses formed by the extremely diverse INs, many of these critical synaptic parameters seem to be alike. For example, hippocampal INs elicit postsynaptic responses that are highly reliable, of large amplitude, and predominantly show short-term depression (9–15). This type of synaptic transmission may be essential for INs synchronizing a large population of PCs (16). However, variability of these synaptic properties has been suggested to be beneficial for stabilizing the network (17). Furthermore, INs also convey autonomic, motivational, and emotional impact on hippocampal information processing, and this type of inhibition is supposed to be easily modifiable (18). In this article, we tested whether all GABAergic synaptic connections in the rat hippocampus were indeed highly reliable with apparent lack of transmission failures; or whether the output of an IN could be dramatically altered, implying a switch in their contribution to network behaviors.

Methods

Slice Preparation and Electrophysiological Recordings. Horizontal hippocampal slices were prepared from 13- to 19-day-old male Wistar rats (15.9 ± 0.3 days, $n = 26$) as described earlier (19). After 1.5 to 6 h of incubation, the slices were transferred to a recording chamber where they were continuously perfused with an aCSF (containing 126 mM NaCl, 2.5 mM KCl, 25 mM glucose, 1.25 mM NaH_2PO_4, 24 mM $NaHCO_3$, 2 mM $MgCl_2$, 2 mM $CaCl_2$, and 3 mM kynurenic acid, pH 7.4). All recordings were performed at 34–36°C. Cannabinoid receptor antagonists and the agonist, the γ-aminobutyric acid type B ($GABA_B$) receptor antagonist, were dissolved in DMSO (a final concentration of 0.1%) that itself had no effect on the synaptic responses ($n = 12$ pairs). Whole-cell current-clamp recordings were carried out from INs by using a potassium gluconate-based intracellular solution, containing 130 mM potassium gluconate, 5 mM KCl, 2 mM $MgCl_2$, 0.05 mM EGTA, 10 mM Hepes, 2 mM Mg-ATP, 0.4 mM Mg-GTP, 10 mM creatinine phosphate, and 0.013 mM biocytin (pH 7.25; osmolality: 270–290 mmol/kg). Action potentials (APs) were evoked by injecting 2- to 3-ms-long depolarizing currents into the cells. PCs were recorded in the whole-cell voltage-clamp configuration at a holding potential of −80 mV. Recording electrodes for PCs were filled with an internal solution containing 40 mM CsCl, 90 mM potassium gluconate, 1.2 mM NaCl, 1.7 mM $MgCl_2$, 3.5 mM KCl, 0.05 mM EGTA, 10 mM Hepes, 2 mM Mg-ATP, 0.4 mM Mg-GTP, and 10 mM creatinine phosphate (pH 7.25; osmolality: 270–290 mmol/kg). Recordings were digitized (at 20 kHz) and analyzed with an in-house software written in LABVIEW. Recordings were excluded from our analysis if the uncompensated series resistance (R_s) was larger than 20 MΩ or the compensated R_s changed >50%. The R_s remaining after 70% to 90% compensation was 2.6 ± 0.2 MΩ. Compound inhibitory postsynaptic currents (IPSCs) were evoked with a θ-glass-stimulating electrode placed in the border of strata radiatum and pyramidale of the CA1 area and in the stratum pyramidale in the CA3 area. CA1 and CA3 PCs were voltage-clamped and IPSCs were recorded as described above. Significance of differences was evaluated with a t test. Data are given as mean ± SEM.

Anatomical and Neurochemical Identification of the Recorded Cells. For light- and electron microscopic examination of the recorded cells, slices containing biocytin-filled neurons were fixed overnight at 4°C in a fixative containing 4% paraformaldehyde, 1.25% glutaraldehyde, and ≈0.2% picric acid in 0.1 M phosphate buffer (pH 7.4). After resectioning of the slices, 60-μm-thick Vibratome sections were incubated in a 2% solution of avidin-biotinylated HRP complex (ABC; Vector Laboratories, Burlingame, CA) in Tris-buffered saline (pH 7.4) followed by several washes. The enzyme reaction was revealed by 3′3-diaminobenzidine tetrahydrochloride (0.05% solution in Tris-buffered saline) as chromogen and 0.01% H_2O_2 as oxidant. Sections were then postfixed in 0.5% OsO_4, stained in 1% uranyl acetate, dehydrated in graded series of alcohol, and embedded into epoxy resin. The axonal and dendritic patterns of each neuron were analyzed at high magnifications and, in some cells, were recon-

This paper was submitted directly (Track II) to the PNAS office.

Abbreviations: PC, pyramidal cell; IN, interneuron; MFA IN, mossy fiber-associated IN; IPSC, inhibitory postsynaptic current; CCK, cholecystokinin; PV, parvalbumin; GABA, γ-aminobutyric acid; $GABA_A$, GABA type A; $GABA_B$, GABA type B; AP, action potential; CB_1, type 1 cannabinoid receptor; P_r, release probability.

*To whom correspondence should be addressed. E-mail: nusser@koki.hu or losonczy@koki.hu.

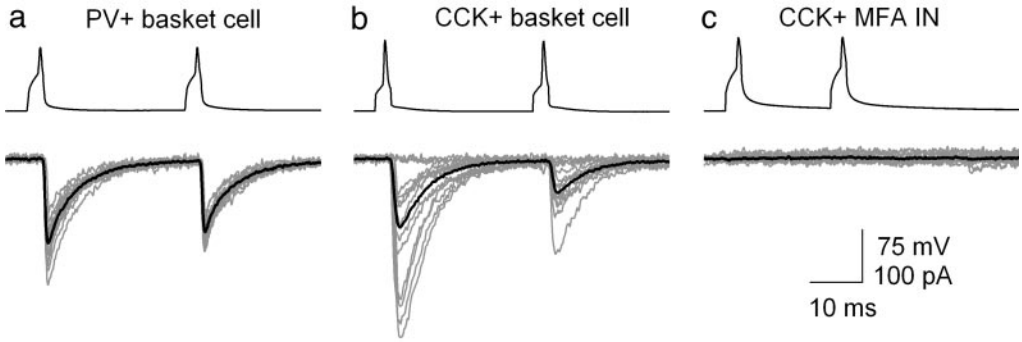

Fig. 1. Unitary IPSCs evoked by different types of GABAergic INs in the CA3 area. (*a*) A PV-positive basket or axo-axonic cell reliably evokes large amplitude postsynaptic responses in a PC. No transmission failure was detected. (*b*) A CCK-immunopositive basket cell generates IPSCs ranging from 0 to ≈600 pA in a postsynaptic PC. The averaged PSC has an amplitude similar to that evoked by the PV+ cell in *a*. (*a* and *b*) Both IPSCs show paired pulse depression. (*c*) Pairs of APs in a CCK-immunopositive MFA IN (cell A753) evoke no postsynaptic responses in a PC. (*a–c*) Fifteen consecutive individual traces are gray and superimposed averaged currents are black. The same scale is used for *a–c*.

structed by using a drawing tube. At sites where the presynaptic axon made close appositions to the postsynaptic cell, serial electron microscopic sections were cut after detailed light microscopic photography. For immunocytochemistry, slices were fixed for 3 h at room temperature in a fixative containing 4% paraformaldehyde, 0.05% glutaraldehyde, and ≈0.2% picric acid in 0.1 M phosphate buffer. Immunoreactivity for parvalbumin (PV) was revealed with a rabbit polyclonal antibody (PV-28; Swant, Bellinzona, Switzerland; diluted 1:1,000 in Tris-buffered saline containing 2% normal goat serum) and for cholecystokinin (CCK) with a mouse mAb (mAb 9303 was provided by the CURE/Digestive Diseases Research Center, Antibody/RIA Core, Los Angeles; diluted 1:1000). The reactions were visualized with a goat anti-rabbit IgG conjugated to Alexa 488 (diluted 1:500 in Tris-buffered saline containing 2% normal goat serum; Molecular Probes), and a goat anti-mouse IgG conjugated to Alexa 594 (diluted 1:500) or Cy3 (1:500; Jackson ImmunoResearch). The biocytin-filled cells were visualized with streptavidin conjugated to Alexa-350 (diluted 1:500). The sections were then mounted in Vectashield (Vector Laboratories) and were subsequently analyzed with a fluorescent microscope.

Results

We carried out simultaneous whole-cell patch-clamp recordings in GABAergic INs and PCs of the hippocampal CA3 area. As reported earlier (9, 10, 12–15), we often found that a single presynaptic AP in GABAergic INs, including PV (Fig. 1*a*)- and CCK (Fig. 1*b*)-immunopositive basket cells, reliably evoked short latency, fast rising, and decaying unitary IPSCs in PCs. However, in some recordings, conventional experimental approaches to test connectivity, such as a single presynaptic AP or a short train of APs (2–10 APs), failed to evoke IPSCs in PCs (Fig. 1*c*). Conventional wisdom would have taken this finding as evidence that the cells were synaptically uncoupled. Yet, when we induced the IN to fire several tens of APs at rates above 50 Hz, a progressively developing PSC was revealed in the PC (Fig. 2*a*). We aimed to characterize functionally this unusual form of synaptic communication by first testing the transmission with single presynaptic APs. Evoking single APs at low frequencies revealed a strikingly high initial failure rate of γ-aminobutyric acid (GABA) release (98.2 ± 0.4%, range: 96% to 100%, n = 11 pairs with >100 trials in each). Given the stochastic occurrence of spontaneous IPSCs in CA3 PCs with a mean frequency of ≈10 Hz, the chance that a spontaneous IPSC will randomly appear within a 1.5-ms time window after the presynaptic AP is 1.5%. This result is exactly what we observed, thus indicating a complete failure of synaptic transmission after single APs. Next we tested the use and frequency dependence of GABA release from such INs by using variable-length AP trains at different frequencies. We assessed the appearance of the first IPSC in the PCs in relation to the presynaptic APs during trains (Fig. 2*b*). On increasing the presynaptic firing rate, the appearance of the first release shifted to earlier APs during the trains (25 Hz: 36 ± 5 AP, n = 7 pairs; 50 Hz: 23 ± 3 AP, n = 8; and 100 Hz: 18 ± 1 AP, n = 28), but still occurred only around the twentieth presynaptic spike at 100 Hz. We also developed a method to statistically evaluate the appearance of postsynaptic responses in PCs. Mean PSCs were calculated in time windows during which the IN fired 10 successive APs at each stimulus frequency. These values were statistically compared to the mean baseline current (due to spontaneous IPSCs) in the absence of presynaptic stimulation (Fig. 2*c*). No significant ($P > 0.05$; paired t test) inward current was found in PCs during the first 70, 50, and 20 APs at 25, 50, and 100 Hz, respectively (Fig. 2*c*). These initially mute synapses, however, released a large number of quanta during the late part of high-frequency (>25 Hz) AP trains. We calculated that as many as 539 ± 113 quanta (total charge 67.6 ± 21.6 pC, n = 12 pairs; quantal charge: 142 ± 25 fC, n = 26) could be released from these axon terminals with 300 APs at 100 Hz. The initial low P_r was not the consequence of an intracellular dialysis during whole-cell recordings, because the pattern of postsynaptic responses and the amplitude of unitary IPSCs did not change during the course of the recordings (see Fig. 6, which is published as supporting information on the PNAS web site).

We next examined whether a specific population from the highly diverse INs may be responsible for such mute connections. We filled the presynaptic INs with biocytin and identified them according to their axodendritic arborizations and neurochemical content. A fully reconstructed representative IN is shown in Fig. 3*b*. The soma is located in stratum lucidum with dendrites spanning all sublayers of the CA3 area. The main axons run parallel with mossy fibers in stratum lucidum, emitting many collaterals in strata lucidum and pyramidale, with significant projections to the hilus. INs with similar axodendritic arborizations have been described (12, 20), and we will refer to them as mossy fiber-associated INs (MFA INs). Sixteen of 18 INs tested showed similar anatomical properties. The remaining two INs had axon arbors predominantly in stratum pyramidale, with similar somatodendritic morphology and hilar axonal projections to those described above. These two cells may be categorized as basket cells. We also found that seven of eight tested cells were immunopositive for the neuropeptide CCK (Fig. 3*a*). The idea that this type of mute connection is a specific feature of MFA INs

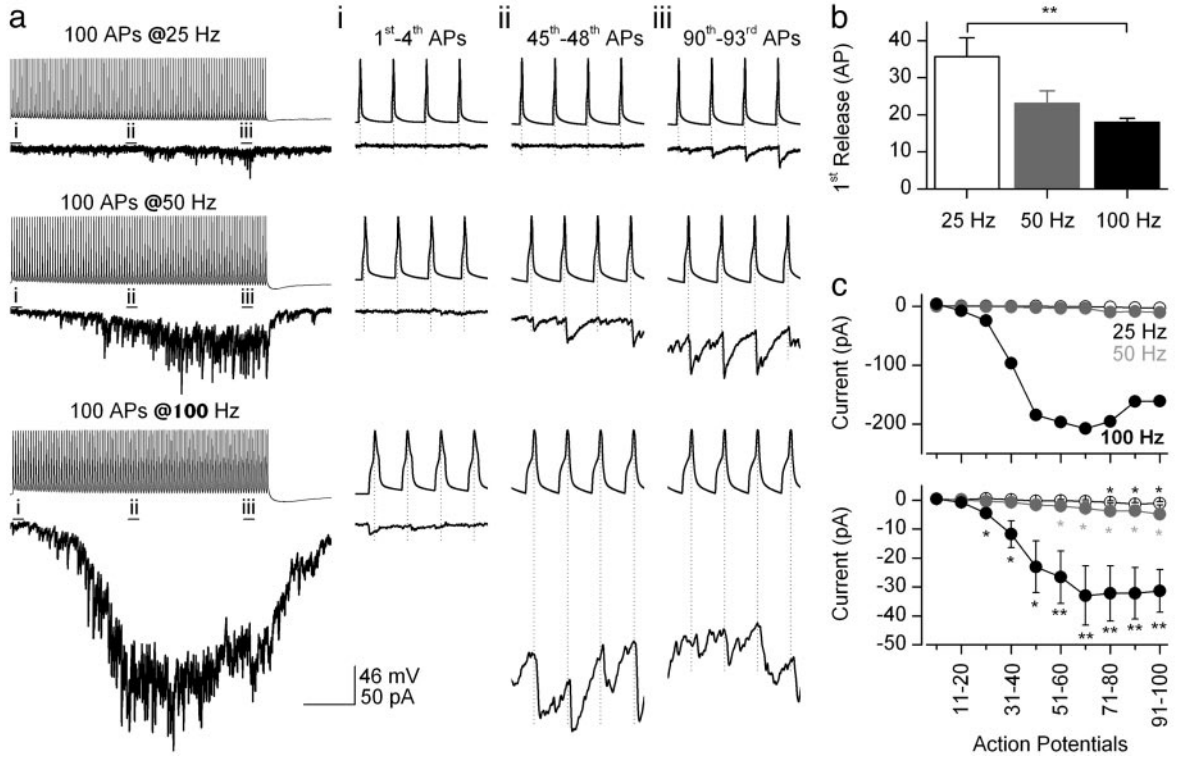

Fig. 2. Use and frequency dependence of GABA release from MFA INs. (*a Left*) Recordings of 100 presynaptic APs (cell A774) and averaged (from 9–10 traces) postsynaptic responses in a PC at three stimulation frequencies. (*Right*) Traces on expanded time scales from the beginning (*i*), middle (*ii*), and end (*iii*) of the stimulus trains. APs at 25 Hz result in postsynaptic responses only at the very end of the AP train. By increasing the presynaptic firing rate to 50 and 100 Hz, the first evoked IPSC appears earlier in the train, but the connection remains still mute during the first ≈10 APs. (Scale bars, 25 Hz: 800 (*Left*) and 60 (*ai*, *aii*, and *aiii*) ms; 50 Hz: 400 (*Left)* and 30 (*ai*, *aii*, and *aiii*) ms; and 100 Hz: 200 (*Left*) and 15 (*ai*, *aii*, and *aiii*) ms. (*b*) Appearance of the first evoked IPSCs at three presynaptic firing frequencies. Means ± SEM are plotted from 7, 8, and 28 pairs at 25, 50, and 100 Hz, respectively. **, $P < 0.01$ using an unpaired *t* test. (*c*) Mean PSCs are plotted over time windows during which the IN fired 10 APs at each stimulus frequency (25 Hz, 400 ms; 50 Hz, 200 ms; and 100 Hz, 100 ms). (*Upper*) Mean currents during trains of 100 APs at three different presynaptic firing rates for the connection shown in *a*. (*Lower*) Summary of several connections (mean ± SEM: 25 Hz, $n = 6$ connections; 50 Hz, $n = 8$ connections; and 100 Hz, $n = 22$ connections). Mean PSCs were statistically compared (paired *t* test; *, $P < 0.05$; **, $P < 0.01$) in the absence (mean baseline current) and in the presence (mean evoked current) of presynaptic stimulation. The mean baseline currents were then subtracted from the evoked currents.

is further supported by our results obtained with consecutive paired recordings. Provided a presynaptic IN had a mute connection onto a PC, the same type of communication was found in all tested (up to four) postsynaptic PCs. Furthermore, as mentioned above, not every CCK+ IN were mute in the CA3 area (Fig. 1*b*), indicating that CCK+ INs are heterogeneous with respect to their initial P_r and short-term plasticity, just as they are according to their input-output relationships and axodendritic arborizations [e.g., basket cells (1, 21), Schaffer collateral-associated INs (22), and MFA INs (12, 20)].

In the next series of experiments, we aimed to provide evidence for the monosynaptic nature of the connections made by MFA INs with PCs. IPSCs evoked by APs in the middle (20–40 APs) of the AP trains, where P_r is low, had short latencies (0.5–1.5 ms; Fig. 3*e*), rapid rise times (20% to 80% rise time = 0.92 ± 0.10 ms, $n = 25$ pairs), and fast exponential decays (τ = 4.8 ± 0.3 ms, $n = 26$; Fig. 3*f*), which is similar to conventional γ-aminobutyric acid type A ($GABA_A$) receptor-mediated IPSCs. Application of the selective $GABA_A$ receptor antagonist SR95531 (>20 μM) completely abolished the postsynaptic responses ($n = 3$ pairs; Fig. 5*a*), confirming that these IPSCs were indeed mediated by $GABA_A$ receptors. Because all experiments were performed in the presence of the ionotropic glutamate receptor antagonist kynurenic acid (3 mM), it is unlikely that the activation of the hippocampal network contributed to the evoked IPSCs. However, to unequivocally ascertain the monosynaptic nature of the IPSCs, we filled both pre- and postsynaptic neurons with biocytin and processed the slices for electron microscopy. After light microscopic reconstruction of the presynaptic IN and the postsynaptic PC, we found close appositions of the presynaptic axon and the proximal apical dendrite of the PC (Fig. 3*c*). Electron microscopic examination revealed that the axon terminals established synaptic junctions on the PC dendrite with ultrastructural features reminiscent to those of conventional symmetrical synapses (Fig. 3*d*). In the two examined pairs, two and three synaptic contacts were found between the pre- and postsynaptic cells, similar to that found earlier (12). Thus, we conclude that this unusual synaptic communication is mediated by conventional chemical synapses with postsynaptic $GABA_A$ receptors.

In our final series of experiments, we attempted to determine the mechanism responsible for the extremely low P_r at these synapses by using specific presynaptic receptor antagonists. It is well established that glutamatergic and GABAergic axon terminals express a wide repertoire of presynaptic auto- and heteroreceptors, all potentially capable of modifying P_r. We tested the contribution of presynaptic metabotropic glutamate (mGluR), $GABA_B$, muscarinic, and cannabinoid receptors, all demonstrated to be present in hippocampal GABAergic axon terminals. First, we tested the potential role of type 1 cannabinoid receptors (CB_1), which are selectively expressed in the axon terminals of CCK+ INs in the hippocampus (23) and underlie depolarization-induced suppression of inhibition (15, 24–29). Application of CB_1 antagonists (10 μM AM251, $n = 6$; or 10 μM

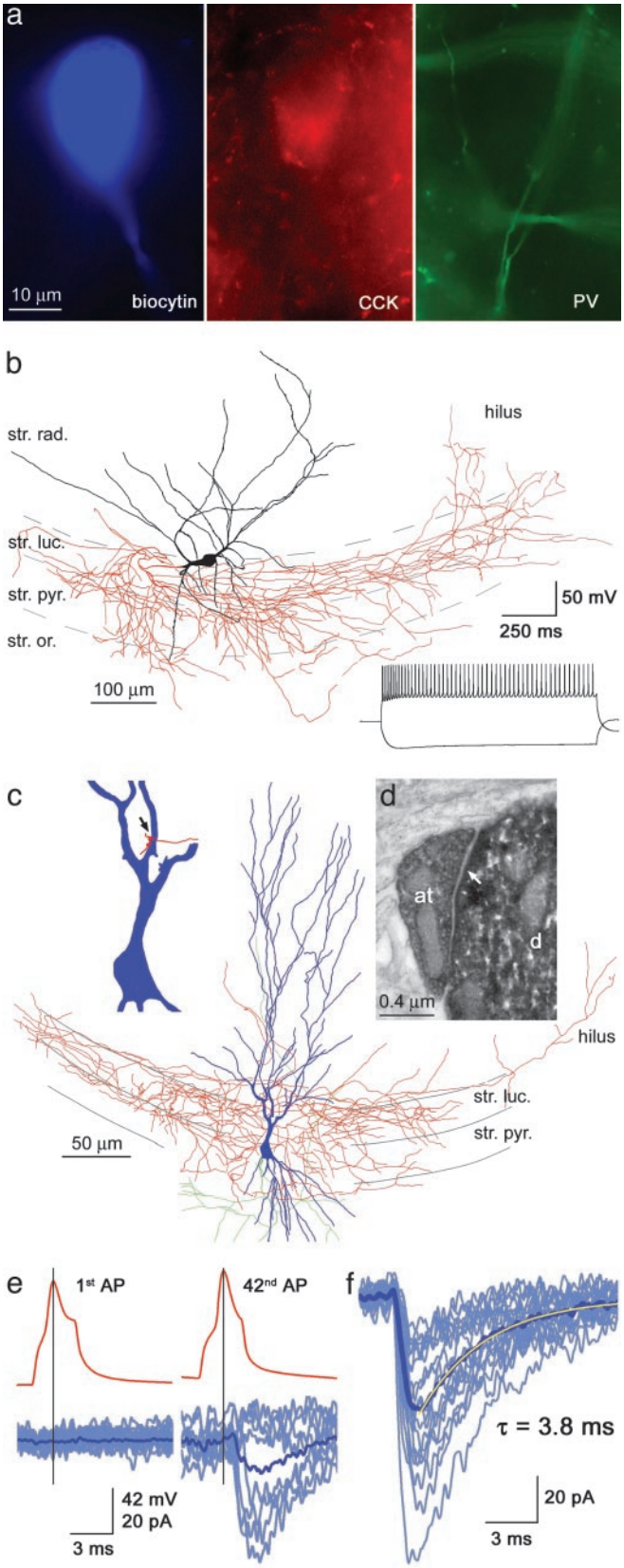

Fig. 3. Morphological identification of presynaptic INs and demonstration of synaptic connections between a presynaptic MFA IN and a postsynaptic PC. (*a*) A biocytin-filled IN (visualized by Alexa 350; *Left*) is immunopositive for CCK (Alexa 594; *Center*) but is immunonegative for PV (Alexa 488; *Right*). (*b*) Reconstruction of a biocytin-labeled IN. Soma and dendrites are black, and the axon is red. Str. or., stratum oriens; str. pyr., stratum pyramidale; str. luc., stratum lucidum; str. rad., stratum radiatum. Note that the main axons of the IN run parallel with the mossy fibers in the stratum lucidum, emitting many collaterals in strata lucidum and pyramidale. (*Inset*) Responses to hyper- and depolarizing current steps (±400 pA). (*c*) Reconstruction of an MFA IN–PC pair. The soma and dendrites of PC are blue, and the axon is green (full reconstruction). Only the axonal arbor of the IN is reconstructed and is red. (*Inset*) The location of close appositions between the IN axon and PC apical dendrite at a higher magnification. (*d*) Electron micrograph of an axon terminal (at) forming synaptic contact on the dendritic shaft (*d*) of the PC. The arrow points to the synaptic junction. (*e*) Electrophysiological properties of the MFA IN–PC pair shown in *c*. The first APs (red) in the presynaptic IN failed to evoke postsynaptic responses, but APs in the middle of 100-Hz trains (e.g., the 42nd AP) were followed by IPSCs in the postsynaptic PC with short latencies (<1.5 ms). Twenty-five and nine consecutive individual traces are in light blue for the first and 42nd APs, respectively. Averages are dark blue. (*f*) Evoked IPSCs (n = 20, light blue) taken from the middle (between 20th and 40th APs) part of 100-Hz trains are aligned for averaging and calculating kinetic parameters of quantal IPSCs. Decay of the averaged IPSC (dark blue) is well fitted by a single exponential function (yellow) with a time constant of 3.8 ms.

SR141716A, $n = 1$) increased the success rate for single presynaptic APs by >20-fold (from 2.2 ± 0.7% to 54.30 ± 11.8%, $P < 0.01$, $n = 7$ pairs with >50 traces in both control and drug periods; Fig. 4*a*). After the antagonist application, the first 10 APs of a high-frequency train evoked a very robust current in PCs (Fig. 4 *b* and *c*; control: 2.2 ± 1.4 pA, $P > 0.05$; antagonist: 39.4 ± 12.7 pA, $n = 7$, $P < 0.05$), demonstrating the conversion of the mute connection into a high-fidelity one. In agreement with the idea that the initial P_r influences the type of short-term plasticity, the CB_1 antagonists also converted the extremely strong facilitation into depression (Fig. 4*a*). Although we have demonstrated that persistently active CB_1 receptors do not mute every CCK-immunopositive IN, we aimed to provide further evidence that the endocannabinoid levels in our preparations are comparable with those in other laboratories (15, 30, 31). Several studies reported that the CB_1 agonist WIN55,212–2 (≈1 μM) resulted in an ≈30% to 40% reduction of the amplitude of compound IPSCs recorded from CA1 PCs (15, 30, 31). We have repeated these experiments in the CA1 area. Fig. 5*c* demonstrates a representative experiment in which 1 μM WIN55,212–2 reduced the amplitude of the evoked IPSCs by 40% (mean reduction 36.8 ± 2.2%, $n = 3$), demonstrating that the levels of endocannabinoids in our preparations are likely to be similar to those in other laboratories. Furthermore, the same experiments were repeated in the CA3 area to exclude the possibility of a hippocampal subregion-specific variation in endocannabinoid levels. Compound IPSCs were reduced by 1 μM WIN55,212–2 (30.4 ± 8.9% reduction, $n = 5$; Fig. 5*d*) to a similar extent to those reported in the CA1 area. The experiment shown in Fig. 5*d* also provides further indication for the coexistence of CB_1-containing axons with initial high and low P_r. The application of the cannabinoid receptor agonist resulted in a 28% reduction of the compound evoked IPSCs in a CA3 PC and the subsequent application of AM251 (10 μM) not only reversed the action of WIN55,212–2 but also resulted in an additional 49% increase in evoked IPSC amplitudes. The most parsimonious explanation of this experiment is that we stimulated some PV+/CB− basket axons, some CCK+/CB_1+ basket axons with high initial P_r, and some CCK+/CB_1+ MFA IN axons with low initial P_r. After the application of the CB_1 agonist, only the CB− axons released transmitter; and, after the application of CB_1 antagonist not only the CB_1+ basket cell axons started to release again but also the mute MFA INs became recruited to the responses. We also performed additional experiments with a mixture of a broad-spectrum mGluR (≈50 μM LY341495), $GABA_B$ (≈10 μM CGP55845), and muscarinic (1 μM atropine) receptor antago-

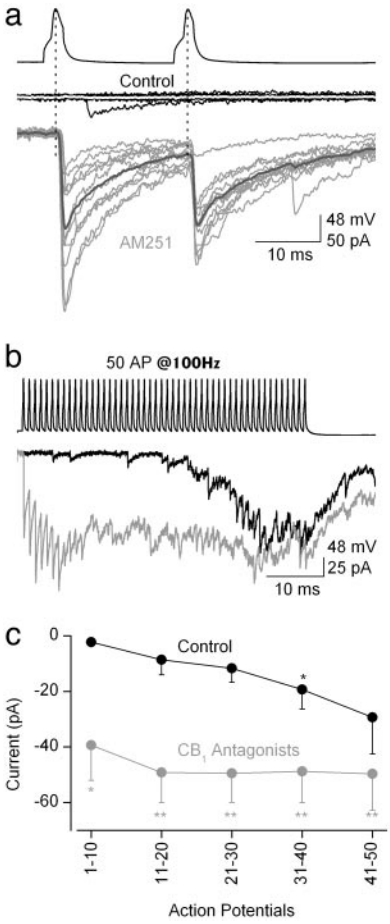

Fig. 4. Persistently active cannabinoid receptors mute MFA INs. (*a*) Two presynaptic APs (50 Hz, top trace) are shown with simultaneously recorded PSCs in a PC before (middle traces) and after (bottom traces) the application of a cannabinoid receptor antagonist (10 μM AM251). Consecutive individual (control: $n = 25$, black; AM251: $n = 12$, gray) and superimposed averaged traces (control: white; AM251: dark gray) are shown for the current records. Fifty APs evoked no IPSC in control but had 100% success rate in the presence of antagonist. (*b*) A high-frequency AP train (50 AP at 100 Hz; top trace) and corresponding averaged postsynaptic responses (bottom traces) in control (black) and in 10 μM AM251 (gray) demonstrate the dramatic change in the reliability of transmission after antagonist application. The same cell pair as shown in *a*. (*c*) Mean $\pm$ SEM of PSCs calculated for 100-ms time windows before (black symbols) and after (gray symbols) the application of CB_1 antagonists (pooled from $n = 6$ pairs in AM251 and $n = 1$ in SR141716A). *, $P < 0.05$; **, $P < 0.01$, paired *t* test.

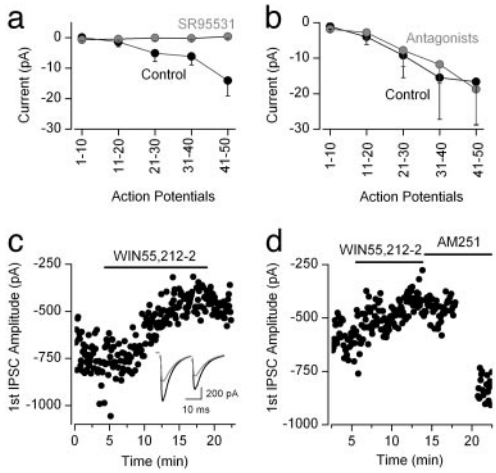

Fig. 5. Pharmacological properties of unitary and evoked IPSCs. (*a*) The selective $GABA_A$ receptor antagonist SR95531 (>20 μM) abolished the PSCs evoked by presynaptic AP trains in MFA INs ($n = 3$). (*b*) A mixture of receptor antagonists (50 μM LY341495, a broad-spectrum mGluR; 10 μM CGP55845, a $GABA_B$; and 1 μM atropine, a muscarinic antagonist) did not affect IPSCs evoked by high-frequency trains of APs (50 APs at 100 Hz) in MFA INs ($n = 4$). (*c*) A CB_1 receptor agonist (1 μM WIN55,212–2) reduces the amplitude of the extracellular-stimulation-evoked IPSCs by 39% in a CA1 PC. (*Inset*) Averaged traces in control (black trace) and in WIN55,212–2 (gray trace). (*d*) Compound IPSCs evoked in CA3 PCs were reduced (28%) by the CB_1 receptor agonist (1 μM WIN55,212–2). Consecutive application of the CB_1 antagonist (10 μM AM251) not only reversed the effect of the agonist but also resulted in an additional 49% increase in IPSC amplitudes. The stimulation had to be stopped for 4 min during the antagonist wash-in period for technical reasons.

nists and found no effect of these antagonists on the initial P_r or on the temporal dynamics of IPSCs (Fig. 5*b*).

Discussion

The major finding of our study is the ability of presynaptic receptors to mute cortical INs in a cell-type-specific manner. Specifically, we have demonstrated that persistently active cannabinoid receptors turn off the output of MFA INs in the hippocampal CA3 area. Although, sustained, high-frequency presynaptic stimulations revealed PSCs in PCs, this mechanism may have little significance *in vivo*. INs are known to fire only few APs at frequencies above 40–50 Hz (5, 32, 33), a pattern that seems to be insufficient to evoke significant GABA release from MFA INs. Unless, MFA INs have a completely different *in vivo* firing pattern, it seems that they have negligible contribution to the network when endocannabinoid levels are similar to those found in our slices. We suggest two possible ways of switching on the synapses formed by these cells. First, the level of endocannabinoids may be reduced by increasing the activity of uptake molecules, or metabolizing enzymes, or by down-regulating their synthesis through a pathway involving phospholipase C activation (25, 34, 35). Alternatively, the plasma membrane density or the affinity of CB_1 receptors may also be down-regulated in an activity-dependent manner. Such an activity-dependent regulation of the surface expression of other G protein-coupled receptors has been shown (36–38), but it remains to be demonstrated for CB_1 receptors. Provided this latter mechanism is in operation, the transmitter P_r and the type of short-term plasticity could be fine-tuned by altering the amount of CB_1 receptors in the plasma membrane of GABAergic axon terminals. The mechanism responsible for the cell-type-specific tonic cannabinoid receptor activity is currently unknown. Because all available CB_1 receptor antagonists are also inverse agonists, our experiments do not allow the discrimination of an endocannabinoid-driven activation of CB_1 receptors vs. a high constitutive activity of the receptors in MFA IN axons. If the former possibility is true, it is still unclear whether a locally elevated endocannabinoid levels around MFA IN axons or a higher density/sensitivity of receptors is responsible for the cell-type specificity of muting. Future experiments with drugs interfering with the synthesis and metabolism of endocannabinoids may help to reveal the mechanisms responsible for the cell-type specificity of INs muting. It is noteworthy that if constitutive receptor activity or higher density/sensitivity of the receptors is responsible for muting MFA INs, this phenomenon should be very similar in the brain of behaving animals in relation to our slices. However, if an elevated endocannabinoid level around MFA IN axons is the reason for the low initial P_r, this may not be identical *in vivo*.

Another prediction of our study is that the output of those cells that are producing reliable postsynaptic responses may be switched off by cannabinoids. CCK-immunopositive INs of the hippocampus include CCK/vasoactive intestinal polypeptide-

positive basket cells (1, 21), CCK+ Schaffer collateral-associated INs (22), and MFA INs. The presence of large amplitude, reliable postsynaptic responses in PCs on the activation of CCK+ basket cells (Fig. 1*b* and refs. 15, 21, 24, and 26), demonstrates that not all CCK-expressing cells are muted by persistently active CB_1 receptors, despite the presence of CB_1 receptors on all CCK-containing axon terminals (23). This finding is further supported by experimental data showing ≈30% to 40% reduction of compound postsynaptic responses after the application of the CB_1 agonist WIN55,212–2 in both the CA1 and CA3 areas (Fig. 5 *c* and *d* and refs. 15, 30, and 31). The release of GABA from CCK-immunopositive basket cells are transiently regulated by endocannabinoids after postsynaptic depolarization (15, 24–29). Depolarization-induced suppression of inhibition lasts for several seconds and only those axon terminals are influenced, which are within few tens of micrometers from the active cells. We suggest that an activity-dependent increase of endocannabinoids through a network-driven high-frequency activity (25, 34), or marijuana/hashish may exert a longer lasting effect through complete muting of these cells, thereby removing them from the neuronal network activities in which they participated.

We thank Drs. T. Freund, I. Mody, and P. Somogyi for their comments on the manuscript. This work was supported by Hungarian Science Foundation Grant T 32329, the Howard Hughes Medical Institute, the Wellcome Trust, the Boehringer Ingelheim Fond, the James S. McDonnell Foundation, and the Japan Science and Technology Corporation.

1. Freund, T. F. & Buzsaki, G. (1996) *Hippocampus* **6,** 347–470.
2. Somogyi, P., Tamas, G., Lujan, R. & Buhl, E. H. (1998) *Brain Res. Rev.* **26,** 113–135.
3. Buzsaki, G. & Chrobak, J. J. (1995) *Curr. Opin. Neurobiol.* **5,** 504–510.
4. McBain, C. J. & Fisahn, A. (2001) *Nat. Rev. Neurosci.* **2,** 11–23.
5. Klausberger, T., Magill, P. J., Marton, L. F., Roberts, J. D., Cobden, P. M., Buzsaki, G. & Somogyi, P. (2003) *Nature* **421,** 844–848.
6. del Castillo, J. & Katz, B. (1954) *J. Physiol. (London)* **124,** 560–573.
7. Dobrunz, L. E. & Stevens, C. F. (1997) *Neuron* **18,** 995–1008.
8. Hanse, E. & Gustafsson, B. (2001) *J. Physiol. (London)* **531,** 467–480.
9. Maccaferri, G., Roberts, J. D., Szucs, P., Cottingham, C. A. & Somogyi, P. (2000) *J. Physiol. (London)* **524,** 91–116.
10. Jensen, K. & Mody, I. (2001) *Nat. Neurosci.* **4,** 975–976.
11. Thomson, A. M., Bannister, A. P., Hughes, D. I. & Pawelzik, H. (2000) *Eur. J. Neurosci.* **12,** 425–436.
12. Vida, I. & Frotscher, M. (2000) *Proc. Natl. Acad. Sci. USA* **97,** 1275–1280.
13. Overstreet, L. S. & Westbrook, G. L. (2003) *J. Neurosci.* **23,** 2618–2626.
14. Kraushaar, U. & Jonas, P. (2000) *J. Neurosci.* **20,** 5594–5607.
15. Wilson, R. I., Kunos, G. & Nicoll, R. A. (2001) *Neuron* **31,** 453–462.
16. Cobb, S. R., Buhl, E. H., Halasy, K., Paulsen, O. & Somogyi, P. (1995) *Nature* **378,** 75–78.
17. Aradi, I., Santhakumar, V., Chen, K. & Soltesz, I. (2002) *Neuropharmacology* **43,** 511–522.
18. Freund, T. F. (2003) *Trends Neurosci.* **26,** 489–495.
19. Losonczy, A., Somogyi, P. & Nusser, Z. (2003) *J. Neurophysiol.* **89,** 1910–1919.
20. Gulyas, A. I., Miles, R., Hajos, N. & Freund, T. F. (1993) *Eur. J. Neurosci.* **5,** 1729–1751.
21. Pawelzik, H., Hughes, D. I. & Thomson, A. M. (2002) *J. Comp. Neurol.* **443,** 346–367.
22. Cope, D. W., Maccaferri, G., Marton, L. F., Roberts, J. D., Cobden, P. M. & Somogyi, P. (2002) *Neuroscience* **109,** 63–80.
23. Katona, I., Sperlagh, B., Sik, A., Kafalvi, A., Vizi, E. S., Mackie, K. & Freund, T. F. (1999) *J. Neurosci.* **19,** 4544–4558.
24. Wilson, R. I. & Nicoll, R. A. (2001) *Nature* **410,** 588–592.
25. Varma, N., Carlson, G. C., Ledent, C. & Alger, B. E. (2001) *J. Neurosci.* **21,** RC188.
26. Ohno-Shosaku, T., Maejima, T. & Kano, M. (2001) *Neuron* **29,** 729–738.
27. Kreitzer, A. C. & Regehr, W. G. (2002) *Curr. Opin. Neurobiol.* **12,** 324–330.
28. Diana, M. A., Levenes, C., Mackie, K. & Marty, A. (2002) *J. Neurosci.* **22,** 200–208.
29. Kim, J., Isokawa, M., Ledent, C. & Alger, B. E. (2002) *J. Neurosci.* **22,** 10182–10191.
30. Hajos, N., Katona, I., Naiem, S. S., MacKie, K., Ledent, C., Mody, I. & Freund, T. F. (2000) *Eur. J. Neurosci.* **12,** 3239–3249.
31. Hoffman, A. F. & Lupica, C. R. (2000) *J. Neurosci.* **20,** 2470–2479.
32. Buzsaki, G. (2002) *Neuron* **33,** 325–340.
33. Csicsvari, J., Hirase, H., Czurko, A., Mamiya, A. & Buzsaki, G. (1999) *J. Neurosci.* **19,** 274–287.
34. Chevaleyre, V. & Castillo, P. E. (2003) *Neuron* **38,** 461–472.
35. Freund, T. F., Katona, I. & Piomelli, D. (2003) *Physiol. Rev.* **83,** 1017–1066.
36. Minami, I., Kengaku, M., Smitt, P. S., Shigemoto, R. & Hirano, T. (2003) *Eur. J. Neurosci.* **17,** 1023–1032.
37. Marvizon, J. C., Martinez, V., Grady, E. F., Bunnett, N. W. & Mayer, E. A. (1997) *J. Neurosci.* **17,** 8129–8136.
38. Flugge, G. (2000) *Int. Rev. Cytol.* **195,** 145–213.